

Spud-can penetration depending on soil properties: Comparison between numerical simulation and physical model test

Dong-Seop Han¹ and Moo-Hyun Kim^{*2}

¹R&D Center, Remitite Co. Ltd., Kyeongnam, South Korea

²Ocean Engineering Department, Texas A&M University, College Station, Texas, USA

(Received April 3, 2017, Revised May 12, 2017, Accepted May 15, 2017)

Abstract. Spud-can is used for fixing jack-up rig on seabed. It needs to be inserted up to the required depth during the installation process to secure enough soil reaction and prevent overturning accidents. On the other hand, it should be extracted from seabed soils as fast as possible during the extraction process to minimize the corresponding operational cost. To achieve such goals, spud-can may be equipped with water-jetting system including monitoring and control. To develop such a smart spud-can, a reliable numerical simulation tool is essential and it has also to be validated against physical model tests. In this regard, authors developed a numerical simulation tool by using a commercial program ANSYS with extended Drucker-Prager (EDP) formula. Authors also conducted small-scale (1/100) physical model tests for verification and calibration purpose. By using the numerical model, a systematic parametric study is conducted both for sand and K(kaolin)-clay with varying important soil parameters and the best estimated soil properties of the physical test are deduced. Then, by using the selected soil properties, the numerical and experimental results for a sand/K-clay multi-layer case are cross-checked to show reasonably good agreement. The validated numerical model will be useful in the next-stage study which includes controllable water-jetting.

Keywords: jack-up platform; smart spud-can; 1/100 physical model test; numerical simulation; parametric study; SSI (Soil-Structure Interaction); soil properties/resistance

1. Introduction

Spud-cans are located at the bottom of jack-up legs and used for temporarily fixing a jack-up platform on seabed. Generally, it should be inserted up to the required depth (e.g., in case of surficial sand, at least half of the spud-can height) during the installation process to secure enough soil reaction and prevent overturning accident. When the seabed is clay, the spud-can typically penetrates much deeper. Then, when service is done, it needs to be extracted from the deep burial position as fast as possible during the extraction process to minimize the operational cost. Also, it should properly function in response to variable sea conditions, soil property changes due to scouring and earthquake, and structural dynamic loadings during the operation process (e.g., DNV codes (2012)).

The soil condition of seabed is largely categorized as the surficial-clay and surficial-sand conditions with multiple layers of similar or other soils below them. In the case of surficial-sand

*Corresponding author, Professor, E-mail: m-kim3@tamu.edu

condition, enough soil reaction is reached even with shallow penetration but it may not be enough for overturning stability. The typically shallow penetration does not cause any serious problem during the extraction process. In the surficial-clay condition, it is relatively easy to insert the spud-can up to the enough depth during the installation process, but it is not easy to extract it from the deep position. In order to solve these problems, spud-cans with water jetting system are to be used (Zhao *et al.* 2011, Qiu *et al.* 2012, Tho *et al.* 2012, Yu *et al.* 2012). If a spud-can with a smart water-jetting system with monitoring and control is developed (e.g., Han *et al.* 2014, 2015), the operational effectiveness can be maximized regardless of seabed soil conditions.

To develop a smart spud-can with monitoring and control, controllable leg-driving system or water-jetting system may be used. They should function properly at each operational phase depending on soil-property changes. For this, the water-jetting effect on the soil reaction in the respective soil conditions needs to be analyzed and the corresponding suitable control methods during various operational phases have to be developed. Many studies on the soil-reaction change due to water jetting have been conducted either by model testing or numerical simulation (Leung 2005, Purwana *et al.* 2006, Bienen *et al.* 2009, Gaudin *et al.* 2011, Duan *et al.* 2013). However, comparisons and verifications between the physical and numerical models for various soil conditions are still very rare. In this regard, a preliminary study is conducted to verify the usefulness of a numerical-simulation technique aiming at the development of the smart spud-can system. To verify the numerical model, small-scale model tests are conducted. The soil properties used in the experiment without water jetting are first calibrated through comparisons between model test and numerical simulation. The changes of spud-can behaviors and penetration depths depending on various soil properties are also illustrated through a systematic parametric investigation.

In this study, the most important soil properties used for physical testing are deduced through comparisons of numerically simulated soil reactions against model-test results. Three soil conditions are used for the numerical simulations and model tests i.e., sand only layer, K-clay only layer, and multi-layer with sand overlaying K-clay. First, the soil reactions according to the penetration depth in the three soil conditions are measured from the 1/100-scale model test. Next, the soil-structure interaction (SSI) analyses are carried out for the same conditions of testing, and the sand and K-clay soil properties are deduced after comparing the experimental and simulation results. The SSI analysis was performed by using the extended Drucker-Prager (EDP) equation and the commercial FEM program ANSYS (2012). Lastly, to verify the numerical model for multi-layer case, the numerical simulation is applied to the sand overlaying K-clay, and the results are checked correctly against the corresponding measurement. The validated numerical model is further applied to the simulation of a spud-can with controllable water-jetting.

2. 1/100-Scale model test

2.1 Test equipment

The test-bed for performance test largely consists of a loading actuator, a loading frame, a container containing soil, a spud-can model as shown in Fig. 1. Also, a load cell for measuring the soil reaction and a potentiometer for measuring the vertical displacement of the spud-can are attached in the test-bed. The spud-can selected here consists of an approximated inverted cone with the maximum diameter of 120 mm and height of 40mm (1/100 scale), and its material is

plexiglass. A loading actuator is a double-action type with maximum force of 1ton and maximum stretching length of 250 mm. A container has an inner capacity of $\phi 500 \times 500$ mm to minimize the effect of the side wall and the bottom. So, the minimum vertical distance between the spud-can and the bottom of the container is set as 200 mm.

2.2 Test condition

For the test, three soil conditions are selected, namely sand only, K-clay only, and sand overlaying K-clay, as shown in Fig. 2. The sand sample is the fine sand with granular size of 0.4~0.6mm. The K-clay sample is normally consolidated clay constituted from kaolin clay. The dry kaolin powder was mixed with water to produce clay slurry at a water content of 120%. The experiment reported in this paper was done without static water above soil. The penetration testing is performed in the order of the sand layer, the K-clay layer, and the sand/K-clay multi-layers. Each case is repeated three times in the same condition to minimize the relevant bias. The soil reaction according to the penetration depth is measured for each soil condition. In the present study, we did not intend to correctly scale any prototype soils in the ocean. Instead, we numerically modeled the physical test as reasonable as possible and tried to best estimate the key soil parameters through extensive parametric comparisons against experimental results to see whether the numerical simulations can reproduce the key physics of soil-structure interactions. Of course, the selected key soil properties were checked to see whether they are within reasonable range. In summary, we numerically model the model test so that the same numerical simulation method can be applied to prototype cases with given soil properties.

2.3 Results of test

The soil reactions are measured as a function of penetration depth in each soil condition. The typical results are shown in Fig. 3. The variability of the K-clay case is larger than that of the sand case but it is still within reasonable band width. The reaction force of the sand layer is generally much greater than that of K-clay layer, as expected. The smaller soil reaction corresponds to larger penetration depth for given platform weight. The larger reaction force results in shallower penetration. When sand overlays K-clay, its reaction strength is significantly reduced compared to the sand-only case.

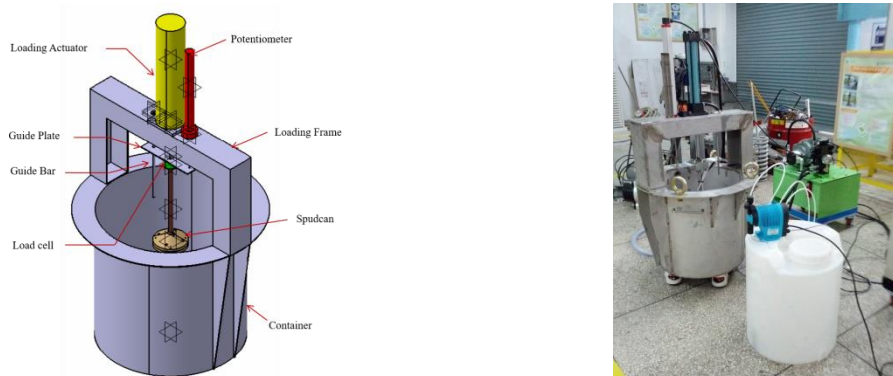


Fig. 1 Test bed for performance test



Fig. 2 Soil conditions for performance test

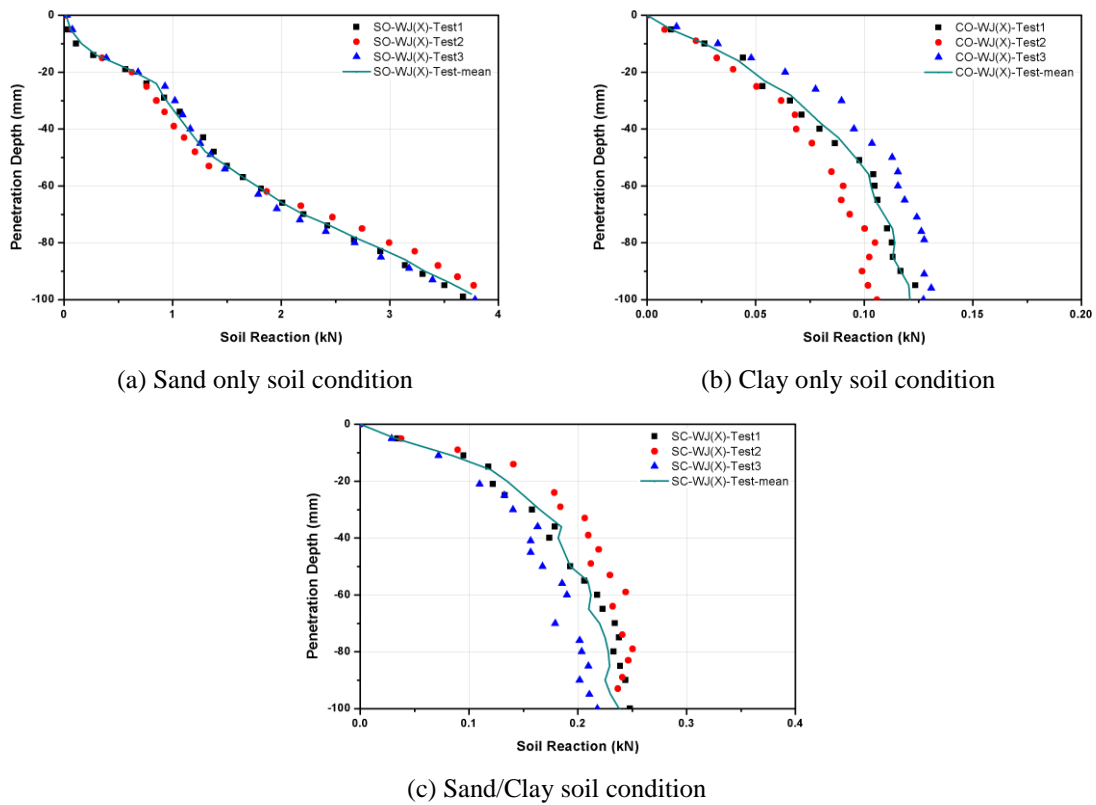


Fig. 3 Soil reactions as function of penetration depth in each soil condition

As shown in Fig. 3, the first mean yield reaction (characterized by large displacement with small force increment, sometimes called punch-through failure) measured through the testing is 0.8 kN in sand layer, 0.1 kN in K-clay layer, and 0.18 kN in sand/K-clay multi-layers, respectively i.e., the first yield reactions in sand layer and in sand/K-clay multi-layers are about 8-times and 2-times larger than that of K-clay layer only. This explains why the spud-can typically penetrates much deeper in the case of clay layer.

3. SSI Analysis for the model

The purpose of SSI analysis is to analyze the soil reaction depending on various soil properties so that the numerical-simulation model can be used to best predict the spud-can penetration depth for the given soil conditions. The most relevant soil parameters are tip resistance (q_c) and equivalent internal friction angle (φ) for sand layer and undrained shear strength (c_u) and cohesion (c) for clay layer. A series of numerical simulations are conducted for various soil parameters to find the best-matched soil properties used in the model tests. Also, we can verify the typical behaviors of the spud-can for the best-matched parameters against the model-test results.

3.1 Basic theory

Extended Drucker-Prager (EDP) theory: The extended Drucker-Prager (EDP) material model includes yield criteria and corresponding flow potentials similar to those of the classic Drucker-Prager model commonly used for geomaterials with cohesion and internal friction. The EDP linear-yield criterion can be expressed as below (Kai *et al.* 2009)

$$t = p \tan \beta + d \quad (1)$$

Where t is the deviatoric stress (stresses- $\sigma_x, \sigma_y, \sigma_z$; yield stress- σ_{yc}), $p = (\sigma_x + \sigma_y + \sigma_z)/3$, $d = (1 - \tan \beta/3)\sigma_{yc}$, and $\tan \beta = 3\sqrt{3}\alpha$, $d = \sqrt{3}\kappa$. Then, the material parameters of soil α and κ in Drucker-Prager model can be obtained as follows

$$\alpha = \frac{2 \sin \varphi}{\sqrt{3}(3 - \sin \varphi)}, \quad \kappa = \frac{6c \cos \varphi}{\sqrt{3}(3 - \sin \varphi)}, \quad c \text{ is the cohesion, } \varphi \text{ is the internal friction angle of soil.}$$

The EDP linear plastic flow potential form can be expressed as below

$$t = p \tan \beta' \quad (2)$$

where $\tan \beta' = 3\sqrt{3}\alpha'$ and $\alpha' = \frac{2 \sin \psi}{\sqrt{3}(3 - \sin \psi)}$, ψ is the dilation angle.

3.2 Analytical/Numerical spud-can-soil model

Spud-can modeling The spud-can model selected here consists of an approximated inverted cone with the maximum diameter of 120 mm. Its material is made from plexiglass that behaves elastically. The jetting nozzles are located close to the outside of the spud-can because the penetration depth critically depends on the shear resistance of a soil around the outer edge of the spud-can. Fig. 4 shows the schematics of the spud-can. The spud-can has the water-jetting system either upwards or downwards. The flowrate can be controlled by pump.

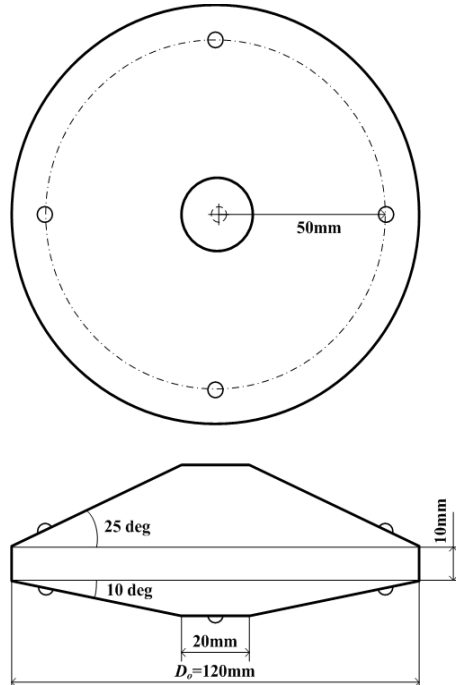


Fig. 4 Schematics of the spud-can

Table 1 Soil properties in model test without water jetting by comparing measurement with SSI analysis

Soil type	tip resistance q_c (MPa)	undrained shear strength c_u (kPa)	Shear strength parameter	
			cohesion c (kPa)	Internal friction angle ϕ (deg)
SAND – WJ(X)	0.1	-	1	26
K-CLAY – WJ(X)	-	0.14	0.8	0

Soil modeling There are two soils used in the experiments (sand and K-clay), whose properties are summarized in Table 1. The Elastic modulus (E) is taken approximately $4 \times q_c$ (for sand) and $200 \times c_u$ (for K-clay), where q_c is the tip resistance from the CPT data and C_u is the undrained shear strength of K-clay. Poisson's ratios (ν) are 0.3 (for sand) and 0.49 (for K-clay), respectively. The dilatation angle (ψ) for sand is equal to the internal friction angle (ϕ) for the Mohr-Coulomb (MC) model. The Drucker-Prager (DP) model is derived from the MC model. In this study, Extended Drucker-Prager (EDP) model is used (Kai *et al.* 2009, Zhao *et al.* 2011). The estimated sand properties reasonably match with typical sand properties of the given granular size. The specific weights γ of the sand and K-clay are $9.0(\text{kN/m}^3)$ and $8.7(\text{kN/m}^3)$.

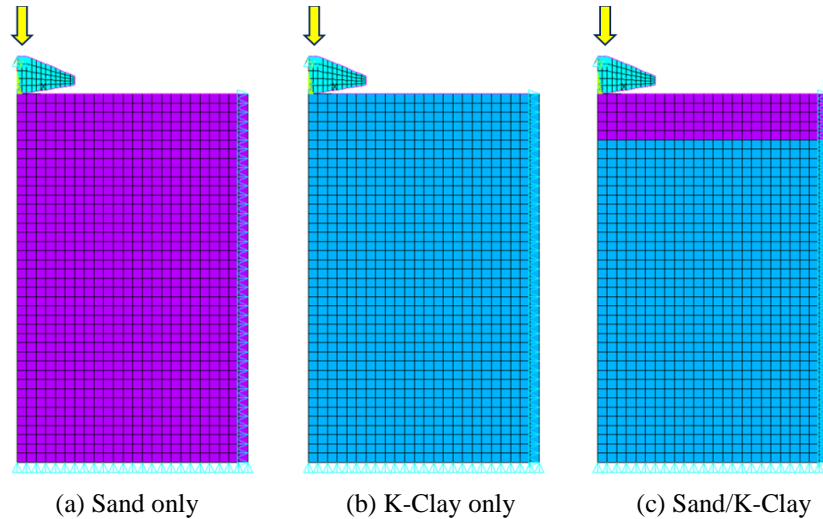


Fig. 5 Meshed shape and boundary condition for SSI analysis

Soil-structure interaction (SSI) modeling The soil-structure interaction is simulated by the surface-to-surface contact pair interaction. The spud-can is selected as a contact surface and the soil as a target surface. The friction coefficient μ between the spud-can surface and soil is set up as 0.3 for a sand layer and 0.4 for a K-clay layer. With water jetting, the friction coefficient may vary but the result is not that sensitive to its change. The SSI analysis was carried out by using ANSYS program. The 2D axisymmetric model for the soil-spud-can is used as analysis option. The radial directional d.o.f (u_x) of nodes on the side surface of soil and vertical directional d.o.f (u_y) of nodes on the bottom surface of soil are fixed, respectively. The vertical displacement (u_z) of top of spud-can is pulled down vertically, after applying the gravity. Fig. 5 shows the meshed shapes and boundary conditions for soil-spud-can interaction model (Kellezi *et al.* 2003, Qiu *et al.* 2012). In this study, the Soil-Structure Interaction (SSI) analysis is based on the implicit finite element method produced by ANSYS, for which Lagrangian (L) formulation is supported for mesh solution. When the deformation of grid (aspect ratio) becomes large, the difference between the L formulation and more rigorous Arbitrary Lagrangian-Eulerian (ALE) formulation (Hossain *et al.* 2005) may be increased. Up to that yielding stage, the differences between the two methods are small (Kellezi *et al.* 2003). In this study, the simulation was stopped when it reached that situation. Also, during the penetration process for sand (slightly wet) and K-clay (kaolin powder containing water) in the model test, the overturning (backflow)/crushing of soil over the upper surface of the spudcan was not observed. Instead, the empty space above it remains intact with vertical wall around the hole. Under those circumstances, the use of the present simulation method is valid, which is also supported by the comparisons against experiment.

3.3 Results of SSI analysis

Fig. 6 shows the equivalent plastic strain distribution of soil in each soil condition. During the penetration process, plastic deformation region in sand layer is wider than that in K-clay layer. The

multi-layer case shows rather abrupt change of strain distribution at the sand-Kclay interface. Compared to the sand only case, the spread of strain distribution for the upper-surface sand is constrained by lower clay in the multi-layer case. In the following, to best estimate the soil properties used in the experiments, a series of parametric studies have been conducted for each soil condition. It needs to point out that the model-test soils were not pretreated by centrifuge operation. When treating multi soil layers, no specific boundary conditions are imposed and the node data between sand layer and clay layer are shared. The program handles the transition of materials by itself.

4. Results and discussions

Parametric Study for Sand only condition The most important properties in sand layer are tip resistance (q_c) and internal friction angle (ϕ). In order to evaluate the parameter-dependent variations in sand layer, four combinations of soil properties are adopted to observe the resulting sensitivity by them, as shown in Table 2. The corresponding soil reaction changes according to the soil property combinations are plotted in Fig. 7. The simulation results are also compared with the testing result.

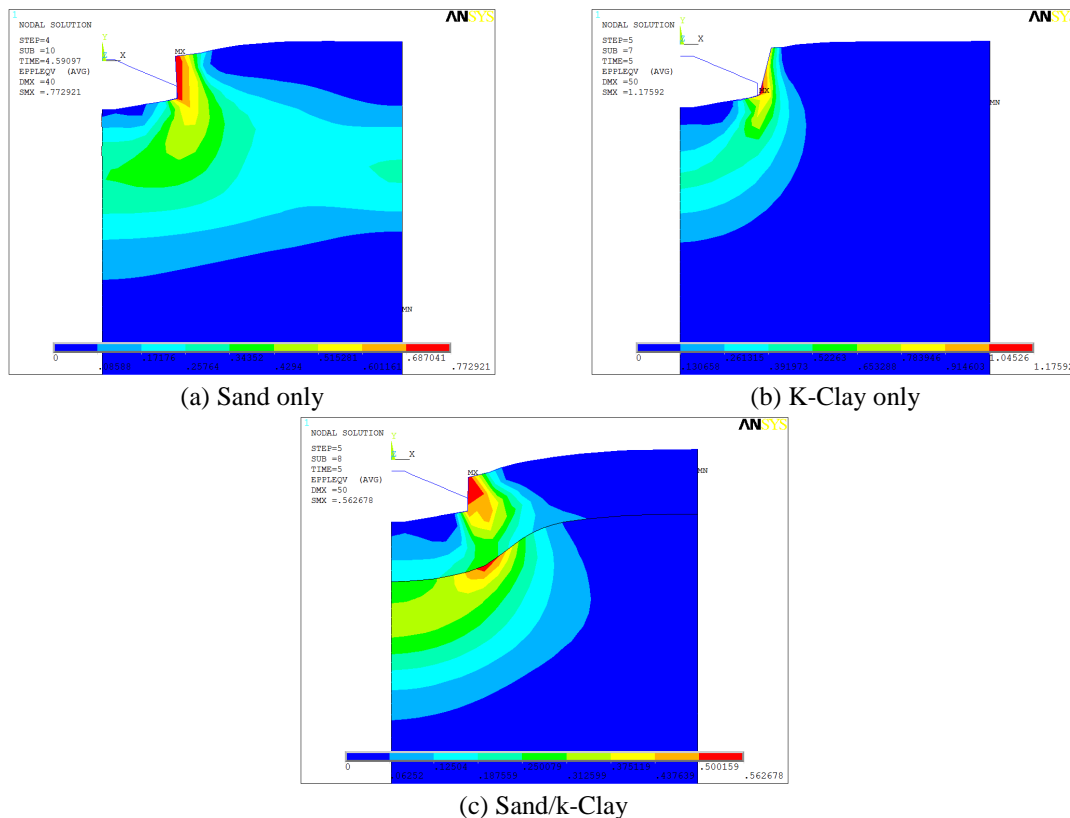


Fig. 6 Equivalent plastic strain distribution of soil in each soil condition

Table 2 Various soil properties for sand layer

Cases	q_c (MPa)	Shear strength parameter	
		c (kPa)	ϕ (deg)
1 (Initial)	3.0	1	30
2	1.0	1	30
3	0.5	1	30
4	0.1	1	30

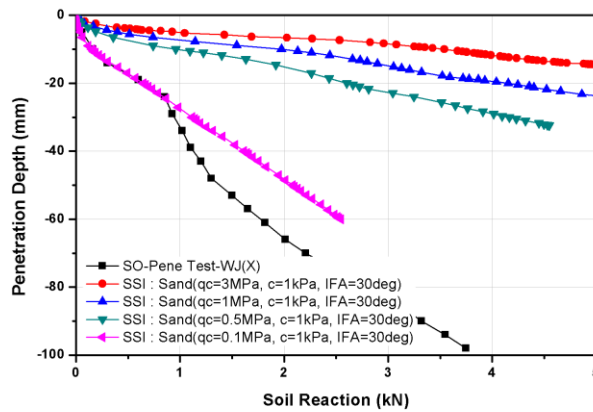


Fig. 7 Soil reaction change according to the soil properties in sand only soil condition

In Fig. 7, the overall slope of the curve for soil reaction is reduced with increasing tip resistance q_c . The initial slope best matches with measurement when q_c is close to 0.1. The later-phase punch-through-like drop, on the other hand, is known to be more related with internal friction angle. When the internal friction angle is reduced to 26 with the chosen $q_c = 0.1$, the behavior after the initial yield can be reproduced (e.g., Han *et al.* 2015), as shown in Fig. 9. Actually the internal friction angle of 26 is the typical value of the fine sand of the granular size used in the experiment.

Parametric Study for K-Clay only condition The most important soil properties in clay layer are undrained shear strength (c_u) and cohesion (c). In order to best estimate the effects of soil-property changes on soil reactions in clay layer, four combinations of soil properties are adopted to observe sensitivity by them, as shown in Table 3. The corresponding soil-reaction changes are shown in Fig. 8. The numerical simulation results are also compared with model-test results.

Table 3 Various soil properties for K-clay layer

Cases	c_u (kPa)	Shear strength parameter	
		c (kPa)	ϕ (deg)
1 (Initial)	10	10	0
2	1	1	0
3	0.5	1	0
4	0.2	1	0

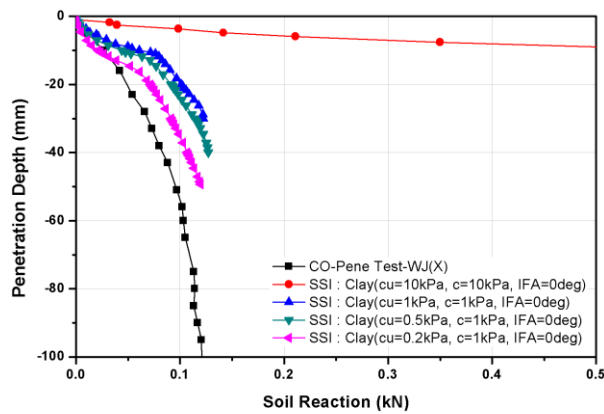


Fig. 8 Soil reaction change according to the soil properties in K-clay only soil condition

In Fig. 8, the overall slopes and curvatures of the curves for soil reaction better match against measurement by reducing the values of undrained shear strength and cohesion as shown in Table 3. By further reducing the c_u and c , better match can be achieved, as shown in Fig. 9.

4.1 Tuning soil properties based on model test

Based on the parametric studies as explained in the previous sections, the soil parameters are further tuned to best match against the measured data. The graphs for the best matched cases between SSI analysis and measurement for the soil reactions as function of penetration depths are given in Fig. 9 for the sand-only and K-clay-only cases. The corresponding soil properties for the cases are shown in Table 1.

Table 1 represents the best estimated soil properties based on the experimental results. The reduced internal friction angle (26 deg.) of experimental fine/loose sand without hardening procedure is actually very close to the value given in the open literature. The undrained shear strength of kaolin containing water is actually very soft with such a small value, which is the typical case without full hardening and drying procedure.

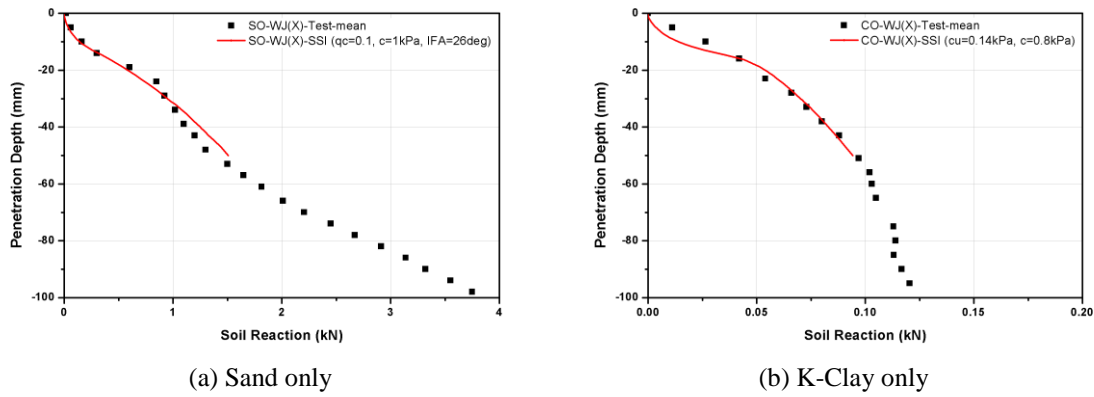


Fig. 9 Comparison of soil reaction between Test and SSI analysis in each soil condition

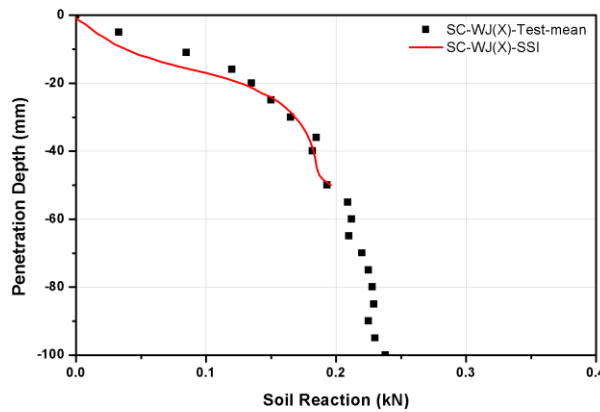


Fig. 10 Comparison of soil reaction as function of penetration depth between model test and SSI analysis in sand/K-clay soil condition

4.2 Further verification of deduced soil properties

In order to further verify the physics of the relevant soil-spudcan interactions and the deduced soil properties of the sand and K-clay, the third case of sand/K-clay combined layers (sand overlaying clay; sand thickness=50 mm, clay thickness=300 mm) is considered. The corresponding SSI analysis for the sand/K-clay multi-layer is carried out by applying the soil properties of Table 1. It is seen that the resistance from the surficial sand layer is significantly weakened due to the K-clay layer below it. The numerical simulation result is compared well with the corresponding experimental data. The comparison is plotted in Fig. 10. The good comparison implies that the developed numerical simulation method along with the selected soil properties works well compared with the small-scale model-test data even for multi-layer cases. This also implies that the proto-type case can be well predicted by the present numerical-simulation technique by using the prototype soil parameters.

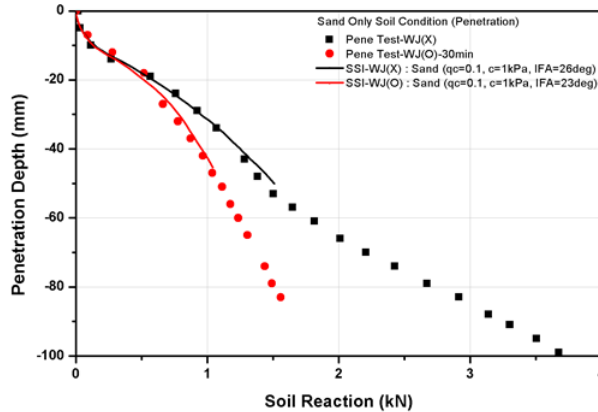


Fig. 11 Comparison of soil reaction due to water jetting between physical model and SSI analysis in sand layer

4.3 Application to Water-Jetting Cases

Finally, let us consider how the present numerical simulation tool can be applied to water-jetting cases. The penetration testing with downward water jetting for sand is performed for 30 minutes with the flow rate of 0.4LPM (litter per minute). After 30 minutes, the sand layer is fully submerged below water free surface. The equivalent internal friction angle tends to gradually decrease with the amount of water jetting until it reaches a critical stage. In Han *et al.* (2014, 2015), the effects of 30 minute water jetting in sand can be well represented by reducing the internal friction angle by about 3 degrees. Fig. 11 shows the comparison of the change of soil reaction due to water jetting between measurement and simulation. It is seen that the water jetting effect can be well represented by the change of equivalent internal friction angle. It is also seen that the water-jetting can effectively be used to increase penetration depth in sand for given structural weight.

5. Conclusions

In this study, both 1/100-scale physical model test and numerical simulation by SSI analysis are carried out to validate the numerical model so that it can be used for the real spud-can design. The soil properties used for the model test are deduced through a systematic parametric study by matching simulation results against experimental results. The three different soil conditions, namely sand only layer, K-clay only layer, and sand/K-clay multi-layers, are considered for both experiment and simulation. In the experiment, the spud-can with outer diameter of 120 mm (1/100 scale) is selected along with the fine sand (granular size of 0.4~0.6 mm) and the kaolin clay with a water content of 120%.

1) The initial yield reaction of the sand layer occurring around 0.8 kN (corresponding penetration depth=22 mm) is much greater than that of K-clay layer occurring around 0.1 kN

(corresponding penetration depth=52 mm). In the case of surface sand overlaying K-clay layer, the initial yield reaction force is about twice that of the K-clay-only case (corresponding penetration depth=40 mm).

2) In the numerical-simulation of sand layer, for any given gravity force, the spud-can penetrates deeper by reducing tip resistance and internal friction angle. In the numerical-simulation of K-clay layer, for any given gravity force, the spud-can penetrates deeper by reducing cohesion and undrained shear strength.

3) The best estimated model-scale soil parameters are deduced from a systematic parametric study. The numerical-simulation model was further validated by comparing the experimental and numerical results for the multi-layer case i.e. surficial sand layer overlaying K-clay layer with the optimized soil parameters. This implies that the present numerical simulation tool can be applied to prototype cases with the prototype soil parameters.

4) The developed simulation program can also be applied to the water-jetting cases by properly selecting the variation of key soil parameters.

Acknowledgements

This research was supported by the InnoPolis Busan under the R&D program supervised by the Korea Ministry of Science, ICT and Future Planning.

References

- ANSYS, Inc. (2012), *ANSYS Mechanical APDL Material Reference*, 47-57.
- Bienen, B., Gaudin, C. and Cassidy, M.J. (2009), "The influence of pull-out load on the efficiency of jetting during spudcan extraction", *Appl. Ocean Res.*, **31**, 202-211.
- Det Norske Veritas AS (2012), *Self-elevating Units*.
- Duan, M., Zhao, J., Wang, J. and Song, L. (2013), "Jetting effect of jackup on actively punching through overlaid sand layer", *J. Offshore Polar Eng.*, **23**(1), 55-62.
- Gaudin, C., Cassidy, M.J., Bienen, B. and Hossain, M.S. (2011), "Recent contributions of geotechnical centrifuge modelling to the understanding of jack-up spudcan behavior", *Ocean Eng.*, **38**, 900-914.
- Han, D.S., Kim, S.J. and Kim, M.H. (2014), "Effect of plate slope and water jetting on the penetration depth of a jack-up spudcan for surficial sand", *Ocean Syst. Eng.*, **4**(4), 263-278.
- Han, D.S., Kim, S.J. and Kim, M.H. (2015), "Effect of water jetting parameters on the behavior of a jack-up spudcan for surficial sand condition", *Ocean Syst. Eng.*, **5**(1), 1-19.
- Hossain, M.S., Hu, Y., Randolph, M.F. and White, D.J. (2005), "Limiting cavity depth for spudcan foundations penetrating clay", *Geotechnique*, **55**(9), 679-690.
- Kai, S.U. and Yin, L.I. (2009), "Discussion of extended Drucker-Prager yield criterion in slope stability analysis", *Proceeding of the Power and Energy Engineering Conference, 2009 APPEEC*.
- Kara, E.M., Meghachou, M. and Aboubekr, N. (2013), "Contribution of particles size ranges to sand friction", *Engineering, Technology & Applied Science Research (ETASR)*, **3**(4), 497-501.
- Kellezi, L. and Stromann, H. (2003), "FEM analysis of jack-up spudcan penetration for multi-layered critical soil conditions", *Proceeding of the BGA International Conference on Foundations*.
- Leung, C.F. (2005), "Challenges in offshore geotechnics in Southeast Asia", *Proceedings of the 16th International Conference on Soil Mechanics and Geotechnical Engineering, 2005 ICSMGE*.
- Purwana, O.A., Leung, C.F. and Chow, Y.K. (2006), "Breakout failure mechanism of jackup spudcan extraction", *Proceedings of the 6th International Conference on Physical Modelling in Geotechnics, 2006*

ICPMG.

- Qiu, G. and Grabe, J. (2012), "Numerical investigation of bearing capacity due to spudcan penetration in sand overlying clay", *Canadian Geotech. J.*, **49**, 1393-1407.
- Tho, K.K., Leung, C.F., Chow, Y.K. and Swaddiwudhipong, S. (2012), "Eulerian finite-element technique for analysis of jack-up spudcan penetration", *Int. J. Geomech. - ASCE*, **12**(1), 64-73.
- Yang, C.K. and Kim, M.H. (2011), "The structural safety assessment of a tie-down system on a tension leg platform during hurricane events", *Ocean Syst. Eng.*, **1**(4), 263-283.
- Yu, L., Hu, Y., Liu, J., Randolph F.M. and Kong, X. (2012), "Numerical study of spudcan penetration in loose sand overlying clay", *J. Comput. Geotech.*, **46**, 1-12.
- Zhao, J., Duan, M., Cao, S., Hu, Z. and Song, L. (2011), "Prediction of spudcan penetration depth in multiple layers with sand overlying clay", *J. Appl. Mech. Mater.*, **52-54**, 995-1002.

PL